

Fabric Defect Detection Using Vision-Based Tactile Sensor

Bin Fang¹, Xingming Long¹, Yifan Zhang², GuoYi Luo¹, Fuchun Sun¹, Huaping Liu¹

Abstract—This paper introduces a new type of system for fabric defect detection – the tactile inspection system. Different from existed visual inspection systems, the proposed system implements a vision-based tactile sensor. The tactile sensor, which mainly consists of a camera, four LEDs, and an elastic sensing layer, captures detailed information about fabric surface structure and ignores the color and pattern. Thus, the ambiguity between a defect and image background related to fabric color and pattern is avoided. To utilize the tactile sensor for fabric inspection, we employ intensity adjustment for image preprocessing, Residual Network with ensemble learning for detecting defects, and uniformity measurement for selecting ideal dataset for model training. An experiment is conducted to verify the performance of the proposed tactile system. The experimental results have demonstrated the feasibility of the proposed system, which performs well in detecting structural defects for various types of fabrics. In addition, the system does not require external light sources, which skips the process of setting up and tuning a lighting environment.

I. INTRODUCTION

Fabric defect detection is a research topic that has been repeatedly investigated for many years. In fact, there are over 2800 papers related to fabric defect detection since 1979 [1], based on Google Scholar search with the key words “fabric defect detection”. The reason is that fabric is one of the necessities which humans rely on extensively; clothing, blankets, and bandages are all made of fabric. Since there is a tremendous amount of demand in fabric, the textile industry flourishes as to satisfy the demand through textile manufacturing. Hence, it is crucial to implement a defect detection system to monitor the quality of fabric in the production lines. Furthermore, the defect detection system can be served as an alert mechanism to prevent further loss of weaving materials for a textile factory [2].

Traditionally, the defect detection system is done by using human eyes, where fabrics are placed on an inspection table and examined by inspectors [3]. However, the accuracy of human inspection is unstable due to fatigue, and it is more challenging for human eyes to detect fine defects. Therefore, automated inspection becomes a popular way for substituting human inspection, as machines are good at repeating a same task without fatigue. Until now, most automated inspection machines are realized by using visual inspection systems,

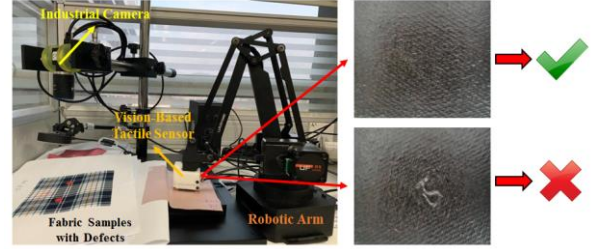


Fig. 1. **Tactile Inspection System.** Our tactile inspection system consists of a vision-based tactile sensor for capturing tactile images, a robotic arm for pressing the tactile sensor onto a fabric, and an industrial camera added for the comparison between tactile images and visual images. We introduce a new tactile inspection system for detecting structural defects on fabrics.

which implement visual sensors such as area scan cameras and line scan cameras. The development of cameras is fairly mature; industrial camera manufacturers such as Basler [4] and Flir [5] provide cameras with high stability and accuracy. The fabric inspection machines developed by Technology companies, such as Uster [6] and Shelton [7], are all based on visual systems. Hence, most algorithms developed for fabric defect detection are also based on visual information. In fact, all the detection algorithms (139 algorithms in total) mentioned in the paper “Automated Fabric Defect Detection – A Review” [8] are all based on visual inspection systems.

Even though various visual based fabric inspection techniques and algorithms have been developed and improved for over 40 years, visual inspection system still encounter challenges such as: 1) numerous types of fabrics; 2) various composition of fabric textures and patterns; 3) similarity in shape between defects and fabric background. The challenges escalate the difficulty for developing fabric inspection algorithms in such a way that most of them are either suitable for a few types of fabric or suitable for various types of fabric but with relatively lower accuracy [8]. Also, the lighting setups of visual inspection systems become complicated due to the three challenges. Depending on the property of fabrics and characteristic of defects, different lighting setups are employed to reveal defects [13], [14].

In order to cope with the aforementioned problems regarding to visual inspection systems, we propose a tactile inspection system, which specialized in detecting structural defects (the definition and examples of structural defects are shown in Fig. 2). The tactile system implements the vision-based tactile sensor [15] for capturing defect information. Currently, vision-based tactile sensors are mostly used for measuring contact force and three-dimensional deformation and load for robots related applications such as grasping [16-19]. In this paper, we introduce a novel implementation of the vision-based tactile sensor for fabric defect detection.

*Corresponding author: fangbin@tsinghua.edu.cn

¹ are from Department of Computer Science and Technology, Tsinghua University, Beijing, China.

² is from Department of Automation, Tsinghua University, Beijing, China.

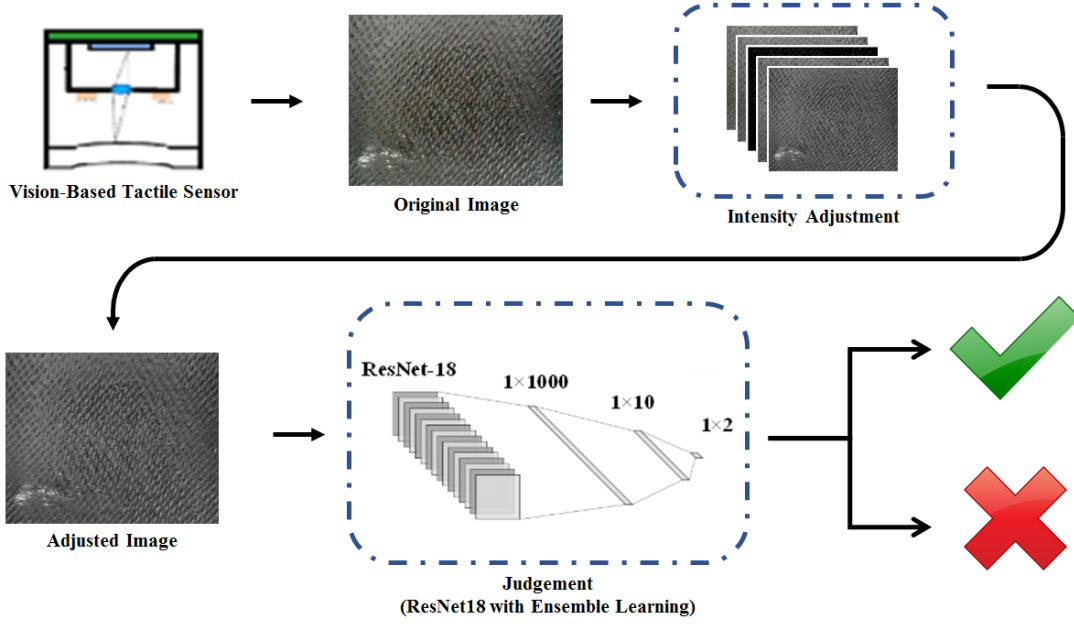


Fig. 4. **Pipeline of Tactile Inspection Algorithm.** The tactile inspection algorithm first receives a tactile image from the tactile sensor. Then, the image is preprocessed by applying intensity adjustment. Finally, the preprocessed image is fed to ResNet18 with ensemble learning which makes a prediction, deciding whether the fabric is defect-free or defective.

The main advantage of the vision-based tactile sensor is that it ignores the color and pattern of a fabric, leaving only the surface and texture information. Hence, the proposed tactile inspection system can prevent the similarity in shape between defects and fabric background related to color and pattern. Furthermore, the tactile system does not require any lighting setup, which saves a tremendous amount of time. For the system's detection algorithm, we employ intensity adjustment for image preprocessing, ResNet18 [12] with ensemble learning for detecting defects, and uniformity measurement for selecting suitable dataset for model training. The main contributions of this research paper can be summarized in the following points:

- A new fabric inspection system that implements a vision-based tactile sensor for detecting structural defects. The new tactile system avoids inspection errors caused by fabric color and pattern and does not required additional lighting setups.
- A defect detection algorithm (combination of intensity adjustment, uniformity measurement, and ResNet18 with ensemble learning) is proposed for utilizing images obtained from a vision-based tactile sensor. Experimental results verify the feasibility of the proposed tactile system, which is able to inspect various types of fabrics with good performance.

The remainder of this paper is organized as follows. Section II is the related work about the research on fabric detection algorithms. Section III gives a basic introduction to the architecture of a vision-based tactile sensor. Section IV provides the detailed content of the proposed detection

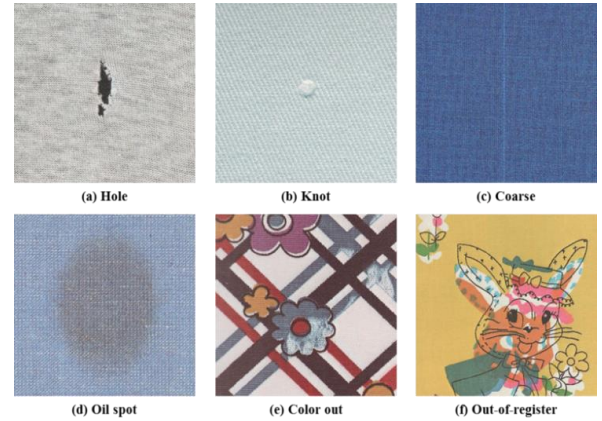


Fig. 2. **Structural and Non-structural Defects.** In this paper, all fabric defects are classified into two categories: structural defects (top row) and non-structural defects (bottom row). Structural defects contain structural deformation of fabrics whereas non-structural defects do not. The images are provided by Cotton Incorporated [9].

algorithm customized for the tactile system. Section V presents the results of the experiment. This paper ends with the conclusion in Section VI.

II. RELATED WORK

The main benefit of the tactile sensor is that it can reduce the complexity of a fabric image by ignoring its color and pattern, as shown in Fig. 3. However, the two main drawbacks are: 1) the intensity of the image is not evenly distributed, which is caused by sensor pressing; 2) the tactile image contains excessive information about fabric texture.

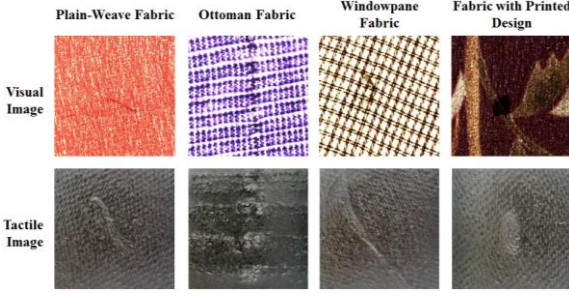


Fig. 3. **Image Comparison of Both System.** The actual images obtained from the industrial camera and the vision-based tactile sensor. There are four sets of fabric images (plain-weave fabric, ottoman fabric, windowpane fabric, and fabric with printed design); each set contains a visual image (top row) and a tactile image (bottom row).

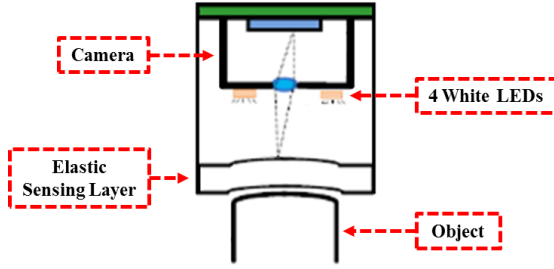


Fig. 5. **Basic structure of vision-based tactile sensor.** The tactile sensor is mainly consisted of an elastic sensing layer for capturing the surface structure of an object, 4 white LEDs for illumination of the elastic sensing layer, and a camera for obtaining the tactile image from the deformation of the elastic sensing layer.

In order to overcome the drawbacks mentioned above, we have done a substantial amount of research on subjects related to fabric defect detection. In general, the defect detection methods for fabric inspection can be classified into seven approaches [8]: 1) statistical, 2) spectral, 3) model-based, 4) learning, 5) structural, 6) hybrid, 7) motif-based.

Based on the research of the seven approaches above, we decided to use spectral approach (Fourier transform [10]) to adjust the intensity throughout the whole image. Fourier transform extracts the texture frequencies in the image, which are used for intensity adjustment. For detecting defects in an irregular texture background, we use learning approach (ResNet18 with ensemble learning). The proposed model is able to learn the difference between defects and fabric texture through model training with human labeled samples. The ensemble learning, which implements a majority vote method, increases the inspection accuracy of the algorithm. The pipeline of the proposed tactile inspection algorithm is illustrated in Fig. 4.

III. ARCHITECTURE OF VISION-BASED TACTILE SENSOR

The tactile sensor we used in the proposed system is a vision-based tactile sensor [15]. The vision-based tactile sensor is mainly consisted of a camera, 4 white LEDs, and an elastic sensing layer, as shown in Fig. 5. When the sensor is pressed onto an object, its elastic sensing layer deforms according to the surface structure of the object. Then, the

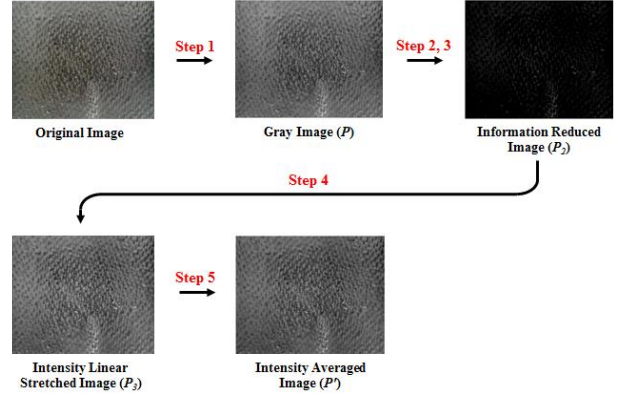


Fig. 6. **Change of Image during Intensity Adjustment.** In the process of intensity adjustment, an original image has gone through multiple procedures to obtain the desired preprocessed image.

camera captures the object surface information through the deformation of the elastic sensing layer. The LEDs provide the illumination of the elastic sensing layer for the camera. Fig. 3 shows the comparison between the visual images and tactile images. Visual images are heavily affected by the color and pattern of a fabric. It is difficult to discriminate the defect from the image background for the windowpane fabric in Fig. 3; its defect has similar features as the image background. Tactile images, on the other hand, avoid this problem by focusing only the surface and textile information

IV. PROPOSED DEFECT DETECTION ALGORITHM

A. Intensity Adjustment

To assure that the intensity of image is evenly distributed, the following steps are performed for intensity adjustment of the original image (the changes of the image during intensity adjustment is illustrated in Fig. 6):

- 1) Convert the original RGB image into a gray image P .
- 2) Apply Fourier transform to convert the image P with the size $M \times N$ into a spectrogram F , and then F is transformed into an amplitude spectrum W through modulation of F :

$$F(u, v) = \frac{1}{MN} \sum_{x=0}^{M-1} \sum_{y=0}^{N-1} P(x, y) e^{-j2\pi(\frac{ux}{M} + \frac{vy}{N})} = |F(u, v)| e^{j\varphi(u, v)} \quad (1)$$

$$W = |F(u, v)| \quad (2)$$

- 3) Find the top five points $(u_1, v_1), (u_2, v_2), (u_3, v_3), (u_4, v_4), (u_5, v_5)$ with the largest values in W and set the values of the corresponding five points in F to 0 to obtain a new spectrogram F' . This process is to remove the low frequency components with the most concentrated energy. F' is converted back to the gray image P_2 :

$$F'(u, v) = \begin{cases} 0, & (u, v) = (u_i, v_i) \text{ and } i = 1, 2, 3, 4, 5 \\ F(u, v), & \text{else} \end{cases} \quad (3)$$

$$P_2(x, y) = \frac{1}{MN} \sum_{u=0}^{M-1} \sum_{v=0}^{N-1} F'(u, v) e^{j2\pi(\frac{ux}{M} + \frac{vy}{N})} \quad (4)$$

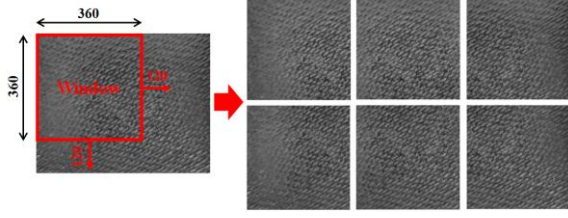


Fig. 7. **Image Block Extraction.** The image size is $480 \times 600 \text{ pixel}^2$ and the extraction window size is $360 \times 360 \text{ pixel}^2$. The movement of the window per step is 120 pixels. There are 6 image blocks extracted from the original image in total.

- 4) Apply linear stretching on P_2 to ensure the range of pixel value in P_2 is 0~255. The new linear stretched image P_3 is obtained by applying the following equation, where $P_2(x_i, y_i)$ is the value of a point (x_i, y_i) in P_2 , p_{min} and p_{max} are the minimum and maximum pixel values in P_2 :

$$P_3(x_i, y_i) = \frac{P_2(x_i, y_i) - p'_{min}}{p'_{max} - p'_{min}} \times 255 \quad (5)$$

- 5) Adjust the average intensity of P_3 to ensure that each preprocessed images have the same average intensity. The average intensity is set to 90 and the final preprocess image is P' :

$$Average = \frac{\sum_{x=0}^{M-1} \sum_{y=0}^{N-1} P_3(x, y)}{MN} \quad (6)$$

$$P'(x_i, y_i) = \frac{90}{Average} \times P_3(x_i, y_i) \quad (7)$$

B. Uniformity Measurement

Uniformity measures the evenness of a fabric texture. If the fabric texture is irregular and contains much noise, its uniformity is low. If the fabric texture is regular and contains less noise, its uniformity is high.

Multiple fixed-size image blocks are extracted from the preprocessed image by moving an $M \times N$ extraction window with a certain horizontal or vertical distance per step, as illustrated in Fig. 7. For n image blocks ($P_1, P_2, P_3, \dots, P_n$) extracted from the original image, each one is processed in the following procedures:

- 1) An image block P_i is first transformed into a spectrogram F_i through 2D Fourier transform, and then transformed into an amplitude spectrum W_i through modulation of the spectrogram. The amplitude spectrum is a 2D image which has the same size as the image block P_i :

$$F_i(u, v) = \frac{1}{MN} \sum_{x=0}^{M-1} \sum_{y=0}^{N-1} P_i(x, y) e^{-j2\pi(\frac{ux}{M} + \frac{vy}{N})} = |F(u, v)| e^{j\varphi(u, v)} \quad (8)$$

$$W_i = |F_i(u, v)| \quad (9)$$

- 2) The point with the largest values in W'_i is set to 0 to remove the low frequency component that has the most concentrated energy. The new amplitude spectrum after low frequency removal is denoted as W'_i .

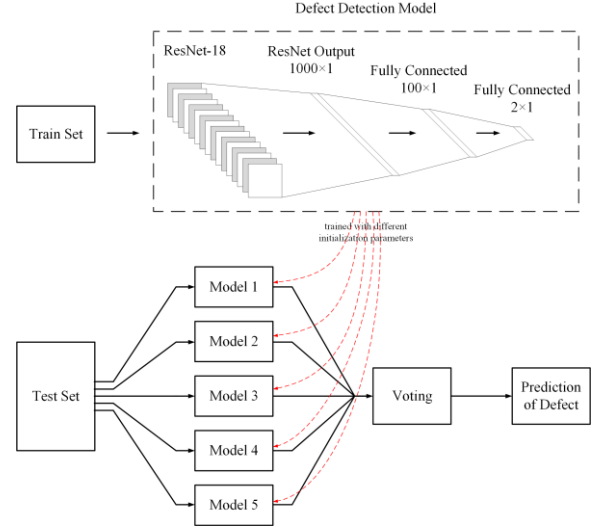


Fig. 8. **Structure of ResNet18 with Ensemble Learning.** The proposed network structure consists of five models that are trained independently; each model contains a ResNet18 and two fully connected layers. A majority vote method is applied to the outputs of the five models to obtain a defect prediction.

- 3) Calculate the sum of all the points in W'_i (Sum_i), and set a $threshold_i$ according to Sum_i . Obtain a set $S_i = \{(x'_{i1}, y'_{i1}), (x'_{i2}, y'_{i2}), (x'_{i3}, y'_{i3}), \dots, (x'_{it_i}, y'_{it_i})\}$ by extracting t_i points in W'_i according to its value from large to small. The value of t_i is selected in the condition when t_i is maximized and the sum of t_i points is not greater than $threshold_i$, as illustrated in the equation below:

$$\sum_{i=1}^{t_i} W'_i(u'_i, v'_i) \leq threshold_i < \sum_{i=1}^{t_i} W'_i(u'_i, v'_i) + \max\{W'_i(C_{W'_i} S_i)\} \quad (10)$$

- 4) Compute the texture frequency ($Frequency_i$) by calculating the summation of the point's weight w_{ij} times its distance d_{ij} from the center c_i of W'_i :

$$Frequency_i = \sum_{j=1}^t w_{ij} d_{ij} \quad (11)$$

where,

$$w_{ij} = \frac{W'(x'_{ij}, y'_{ij})}{\sum_{k=1}^t W'(x'_{ijk}, y'_{ijk})}$$

$$d_{ij} = \sqrt{(x'_{ij} - c)^2 + (y'_{ij} - c)^2}$$

After going through the above procedures, we obtain the texture frequencies of the n image blocks. The uniformity of the entire preprocessed image is obtained by computing the average of the texture frequencies with the removal of the q highest and the q lowest texture frequencies.

C. ResNet18 with Ensemble Learning

For making a defect or defect-free judgement on a fabric image, we implement a network model which is consisted of

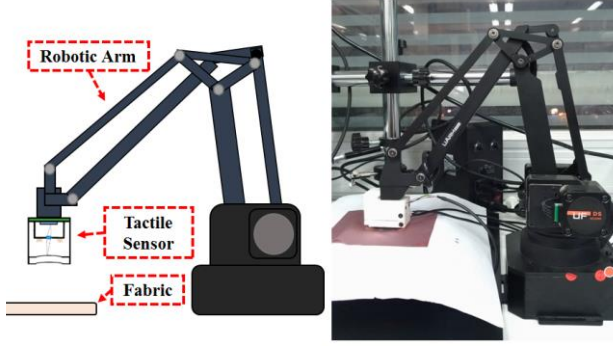


Fig. 10. **Environmental Setup for Tactile Inspection System.** The setup mainly includes a vision-based tactile sensor, a robotic arm, and a fabric.

a ResNet18 and two layers of fully connected layers. To cope with the problem regarding to excessive amount of texture information in tactile images, ensemble learning is introduced to increase the performance of the model. Five individual models, with their parameters initialized randomly, are built and trained independently. When performing fabric inspection, each five models takes in the same preprocessed image and makes a prediction. Finally, a majority vote method is applied to sum up the predictions of the models. In this voting method, if the majority of the models predict the image as defective (e.g. 3 models vote for defective and 2 models vote for defect-free), the image is considered as defective.

The reason we apply ensemble learning instead of using the ResNet18 model directly is that fabric texture affects the performance of the model. Fabric texture distracts the model from discriminating defects from the image background. Thus, it is risky to rely on just one model for detecting defects. Ensemble learning increases the inspection performance by allowing the usage of multiple models; if one model fails to detect a defect, other models might detect it. The entire network structure is shown in Fig. 8.

V. EXPERIMENTAL RESULTS

A. Parameter Setting

In the experiment, we use uArm Swift Pro for the robotic arm, a self-made vision-based tactile sensor in our lab, and Basler MV-CA050-11UC for the industrial camera. The platform of the computer used in the experiments is Windows 10 (i9-9900 CPU).

There are totally 14 types of defect fabrics used in experiment, shown in Fig. 9. Each type of fabric only contains 1 or 2 defect types and its images are taken multiple times with different translation and rotation. All the images are in RGB format and have the size $480 \times 600 \text{ pixel}^2$. For each fabric type, we took roughly 100 defect-free images and 100 defective images; the total amount of images we obtained is 2766 (1367 defect-free and 1399 defective).

For the training of the proposed model, the input image is resized to $288 \times 288 \text{ pixel}^2$, the epoch is set to 20, and the batch size is set to 4. The learning rate begins with 0.02 and gradually decreases through exponential decay; the learning rate is decreased by 10 percent after each epoch. Cross entropy is selected for loss function. Stochastic gradient descent is implemented as network optimizer.

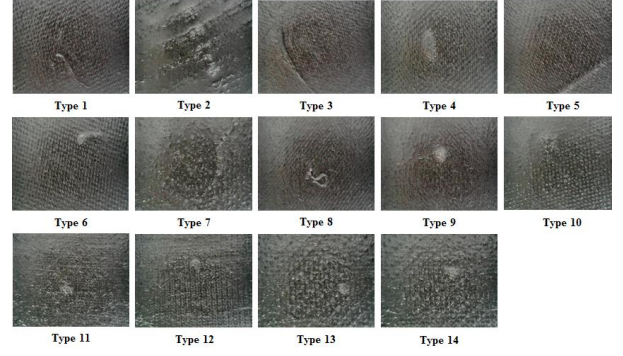


Fig. 9. **Fabric Types.** Actual images obtained from the vision-based tactile sensor.

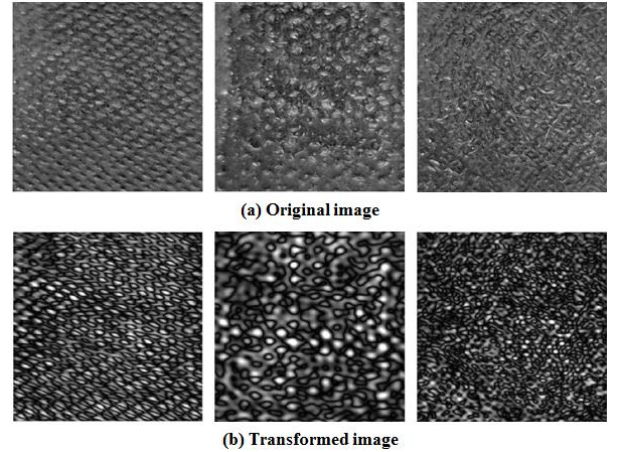


Fig. 11. **Images Before and After Fourier Transform.** (a) Original preprocessed images. (b) Images that have gone through Fourier transform and inverse Fourier transform. For better observation, all the pixel values in the transformed images are multiplied by 5.

B. Environmental Setup

In the tactile inspection system, a vision-based tactile sensor is attached on the end-effector of the robotic arm. The robotic arm moves down the tactile sensor to press it onto a fabric for collecting tactile images. Fig. 10 shows the environmental setup for the proposed tactile inspection system.

C. Fabrics Uniformity Measurements

The uniformities of all the fabrics are measured by using the procedures stated in Section IV – A. We set $threshold_i$ to $Sum_i/40$ for obtaining the texture frequencies for all the 6 image blocks extracted from a preprocessed image. We then applied inverse Fourier transform to reverse back the spectrograms of the image blocks to gray images. From the observation of the original images and the transformed images (shown in Fig. 11), we notice the transformed images can be seen as representations of the fabric texture. This representation verifies the use of texture frequencies for measuring the uniformity of a fabric image. In order to maintain a stable uniformity measuring, the two image blocks

with the highest texture frequencies and the two image blocks with the smallest texture frequencies are discarded. The uniformity is obtained by calculating the average of the texture frequencies of the remaining two image blocks. The measurements of the uniformities for all fabric types are shown in Fig. 12. From the observation of Fig. 12, we noticed that fabric type 2 and 7 have the lowest uniformity in average. This result can be verified by observing the tactile images of type 2 and 7 in Fig. 9; the textures of these two images are much different and uneven from the other ones.

D. Evaluation of ResNet18 with Ensemble Learning

In this experiment, we first separated the dataset based on the fabric uniformity. The fabric types (1, 3, 4, 6, 10, and 12) with higher uniformity are selected into the training set, and the fabric types with lower uniformity (2, 5, 7, 8, 9, 11, 13, and 14) are selected into the testing set. Through this separation, we ensure that texture information does not affect the model too much during the training process, so the model can focus on learning the defect features. In this experiment, we want to evaluate the performance of the proposed algorithm on various types of fabrics.

Two separate tests are running. In the first test, the model takes in original images as input. In the second test, the model takes in intensity-adjusted images. The inspection accuracies of the two separate models are shown in the table below. The accuracy is calculated by dividing the number of samples correctly detected to the total number of samples.

TABLE I
INSPECTION RESULTS OF THE TWO MODEL TESTS

Fabric Type	2	5	7	8	9	11	13	14
<i>Original Image</i>	0.5	1.0	0.5	1.0	1.0	0.971	0.715	0.83
<i>Intensity-Adjusted Image</i>	0.5	0.97	0.51	1.0	1.0	0.976	0.985	0.97

As shown in Table I, the model with original images as input has higher inspection accuracy when inspecting fabrics with high uniformity (type 5, 8, 9, and 11), and has lower inspection accuracy for fabrics with median uniformity (type 13 and 14). However, when the model is provided with intensity-adjusted images instead, its accuracy on fabrics with median uniformity (type 13 and 14) increases. For fabrics with low uniformity (fabric 2 and 7), the inspection result is undesirable.

To evaluate the robustness of the model, another test is conducted. In this test, fabric type 3 and 6 (higher uniformity) in the training set are swapped with fabric type 2 and 7 (lower uniformity) in the testing set. The new training set now has fabric type 1, 2, 4, 7, 10, and 12 and the new testing set has fabric type 3, 5, 6, 8, 9, 11, 13, and 14. The table below shows the result of the new test.

The result in TABLE II indicates that training the model with images that have low uniformity affects the model performance. If the training images contain too much irregular texture information, it is harder for the model to

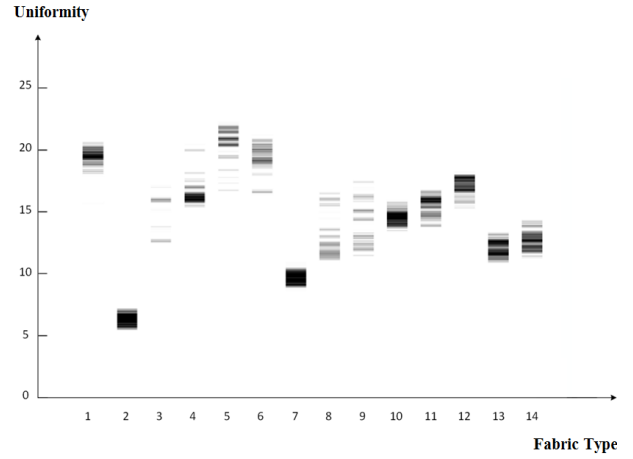


Fig. 12. **Uniformity Measurements for All Fabric Types.** The x-axis is the fabric type number and the y-axis is the uniformity value. Each strip represents the uniformity of a sample in a particular fabric type. The strip becomes darker when multiple strips concentrate in the same area.

learn the defect features. Nevertheless, the overall performance of the model is high even when different types of fabrics are introduced to the model. Thus, this result shows that the proposed model has high robustness.

TABLE II
INSPECTION RESULTS BEFORE AND AFTER SWAPPING

Fabric Type	3	5	6	8	9	11	13	14
<i>Before Swapping</i>	N/A	0.97	N/A	1.0	1.0	0.976	0.985	0.97
<i>After Swapping</i>	1.0	0.97	0.98	0.995	1.0	0.962	0.935	0.975

VI. CONCLUSION

In this paper, we introduce a new tactile inspection system that provides an alternative way for detecting structural defects. Benefiting from the use of a vision-based tactile sensor, the problem regarding to the similarity between the shape of defects and patterns is solved. Furthermore, the tactile system does not require additional lighting setup, which reduces cost and development time. To utilize the tactile sensor, we have proposed a defect detection algorithm. The algorithm employs: 1) intensity adjustment to handle the problem regarding to image intensity which is caused by uneven sensor pressing; 2) uniformity measurement to select suitable fabric images for model training by measuring their texture frequencies; 3) ResNet18 with ensemble learning to perform fabric defect detection with high robustness. Experimental results have indicated that the proposed defect detection algorithm for the tactile system is able to detect structural defects with high accuracy on various types of fabrics that have medium or high uniformity. In our future work, we would like to combine a visual sensor and a tactile sensor to create a multi-modal system for fabric inspection.

ACKNOWLEDGMENT

This work was supported by The Tsinghua University Initiative Scientific Research Program No.2019Z08QCX15.

REFERENCES

- [1] H. Koshimizu, "Fundamental Study On Automatic Fabric Inspection By Computer Image Processing," Proc. SPIE – Imaging Applications for Automated Industrial Inspection and Assembly, vol. 182, Oct. 1979.
- [2] K. Hanbay, M. F. Talu, and Ö. F. Özgüven, "Fabric defect detection systems and methods—A systematic literature review," *Optik*, vol. 127, pp. 11960-11973, 2016.
- [3] A. Kumar, "Computer-Vision-Based Fabric Defect Detection: A Survey," *IEEE Transactions on Industrial Electronics*, vol. 55, no. 1, pp. 348-363, Jan. 2008.
- [4] Basler. (2019). Basler Official Website [Online]. Available: <https://www.baslerweb.com/>
- [5] Flir. (2019). Flir Official Website [Online]. Available: <https://www.flir.com/>
- [6] Uster Technologies. (2019). Fabric Inspection [Online]. Available: <http://www.uster.cn/en/instruments/fabric-inspection/>
- [7] Shelton Vision. (2019). Visual Inspection Systems [Online]. Available: <https://www.sheltonvision.co.uk/visual-inspection-systems/>
- [8] H. Y. T. Ngan, G. K. H. Pang, and N. H. C. Yung, "Automated fabric defect detection – A review," *Image and Vision Computing*, vol. 29, pp. 442-458, 2011.
- [9] Cotton Incorporated. (2020). Standard Fabric Defect Glossary [Online]. Available: www.cottoninc.com/quality-products/textile-resources/fabric-defect-glossary/
- [10] I. N. Sneddon, *Fourier Transforms*, USA, Courier Corporation, 1951.
- [11] C. Neubauer, "Segmentation of defects in textile fabric," in *Proc. IEEE 11th Int'l Conf. Pattern Recognition*, 1992, vol. 1, pp. 688-691.
- [12] K. He, X. Zhang, S. Ren, and J. Sun, "Deep Residual Learning for Image Recognition," in *IEEE Conf. on CVPR*, 2016, pp. 770-778.
- [13] K. Tout, "Automatic Vision System for Surface Inspection and Monitoring: Application to Wheel Inspection," Ph.D. dissertation, Signal and Image Processing, Univ. de technologie de Troyes, French, 2018. Accessed on: Jan. 12, 2020. [Online]. Available: <https://tel.archives-ouvertes.fr/tel-01801803/document>
- [14] Shelton Vision. (2019). Machine Vision Solutions [Online]. Available: <https://www.sheltonvision.co.uk/visual-inspection-systems/machine-vision-solutions/>
- [15] Bin Fang, Funchun Sun, Huaping Liu, A dual-modal vision-based tactile sensor for robotic hand grasping, *International Conference on Robotics and Automation*, 2018, 2483-2488.
- [16] Fuchun Sun, Bin Fang, Huaping Liu, A novel multi-modal tactile sensor design using thermochromic material, *Science China Information Sciences*, 2019, 62(11): 214201.
- [17] Y. Zhang, Z. Kan, Y. Yang, Y. A. Tse, and M. Y. Wang, "Effective Estimation of Contact Force and Torque for Vision-Based Tactile Sensors With Helmholtz–Hodge Decomposition," *IEEE Robotics and Automation Letters*, vol. 4, no. 4, pp. 4094-4101, Oct. 2019.
- [18] C. Sferrazza, and R. D'Andrea, "Transfer Learning for Vision-Based Tactile Sensing," in *IEEE/RSJ International Conf. on Intelligent Robots and Systems (IROS)*, 2019, pp. 7961-7967.
- [19] Bin Fang, Funchun Sun, Huaping Liu, A cross-modal tactile sensor design for measuring robotic grasping forces, *Industrial robot*, 2019, 46(3): 37-44.